M. WEYRAUCH,[1] M.V. RAKOV [2]

[1] Physikalisch-Technische Bundesanstalt
*(Bundesallee 100, D-38116 Braunschweig, Germany)*
[2] Faculty of Physics, Taras Shevchenko National University of Kyiv
*(4, Glushkov Ave., Kyiv 03127, Ukraine)*

PACS 71.27.+a, 05.10.Cc, 02.70.-c, 75.10.Pq

# EFFICIENT MPS ALGORITHM FOR PERIODIC BOUNDARY CONDITIONS AND APPLICATIONS

*We present the implementation of an efficient algorithm for the calculation of the spectrum of one-dimensional quantum systems with periodic boundary conditions. This algorithm is based on a matrix product representation for quantum states (MPS) and a similar representation for Hamiltonians and other operators (MPO). It is significantly more efficient for systems of about 100 sites and more than for small quantum systems. We apply the formalism to calculate the ground state and the first excited state of a spin-1 Heisenberg ring and deduce the size of a Haldane gap. The results are compared to previous high-precision DMRG calculations. Furthermore, we study the spin-1 systems with a biquadratic nearest-neighbor interaction and show the first results of an application to a mesoscopic Hubbard ring of spinless fermions, which carries a persistent current.*

*Keywords:* matrix product representation for quantum states (MPS) and Hamiltonians (MPO), spin-1 Heisenberg ring, density matrix renormalization group (DMRG).

## 1. Introduction

It was recognized early on that the density matrix renormalization group (DMRG) simulations of one-dimensional (1D) quantum systems require significantly more numerical resources for periodic boundary conditions (PBC) than that for open boundary conditions (OBC) [1]. Verstraete, Porras, and Cirac (VPC) [2] addressed this issue, and they proposed an algorithm in terms of matrix product states (MPS), which scales significantly better with the matrix size $m$ of the MPS than the standard DMRG with PBC. However, the intermediate steps of this algorithm require matrices of size $m^2 \times m^2$, and the computer time and memory necessary to determine the improved representation still scale with $m^5$ as compared to $m^3$ for OBC.

This issue was addressed by Pippan, White, and Evertz (PWE) [3], who recognized that, for sufficiently large systems, a much more efficient implementation is possible with the use of a singular value decomposition (SVD) of products of certain transfer matrices. In order to calculate such products with sufficient accuracy, only rather few singular values must be kept.

The usefulness of the improved algorithm was demonstrated in Ref. [3] by a calculation of the ground state of the spin-1 Heisenberg Hamiltonian. The authors showed that the accurate results for the ground-state energy are obtained by a comparison with highly accurate standard DMRG calculations. As a result, it was concluded that, for large enough systems, one obtains an algorithm that scales similarly with $m$ as calculations for systems with OBC.

In the present paper, we extend the PWE algorithm in two respects: first, we propose an implementation of this algorithm in terms of MPS and matrix product operators (MPO). To this end, we define generalized transfer matrices, which are subjected to an SVD. This enables further gains in the efficiency in certain situations. Second, we extend the PWE framework and include the calculation of the excited states of 1D many-body Hamiltonians.

We apply this algorithm to a small collection of spin models (bilinear and biquadratic spin-1), as well as to a spinless fermion model. In the course of these applications, it was found that the number of singular values one must keep depends generally on the matrix size $m$, i.e., the larger $m$, the more singular values must be kept in order to produce high-precision results.

From the MPS representation, it is straightforward to calculate correlation functions and other observ-

ables. The results of such calculations will be presented elsewhere.

## 2. MPS-MPO Formalism for PBC

First, we rewrite the algorithm proposed in Ref. [2] in terms of MPS and MPO: the states of a 1D quantum system of size $N$ (e.g., a spin system) are approximated in terms of a matrix product state (MPS),

$$|\psi\rangle = \mathrm{Tr}\; B^{[1]}_{\sigma_1} \times ... \times B^{[N]}_{\sigma_N} |\sigma_1, ..., \sigma_N\rangle. \quad (1)$$

Here, $\sigma_j$ represent the local degrees of freedom at the site $j$, and each $B^{[j]}_{\sigma_j}$ represents a matrix of size $m \times m$, where $m$ is called the bond dimension. In the algorithm to be described, the elements of these matrices are variational parameters to be adjusted using a suitable optimization procedure. The trace in Eq. (1) ensures periodic boundary conditions and includes a sum over all $\sigma_j$.

Analogously, the operators are written as matrix product operators (MPO)

$$O = \mathrm{Tr}\; W^{[1]}_{\sigma_1,\sigma'_1} ..., W^{[N]}_{\sigma_N,\sigma'_N} |\sigma_1, ..., \sigma_N\rangle\langle\sigma'_1, ..., \sigma'_N|, \quad (2)$$

and the trace includes a sum over all $\sigma_j$ and $\sigma'_j$. Again, each $W^{[1]}_{\sigma,\sigma'}$ represents a matrix of size $m_W \times \times m_W$, i.e., each $W$ is a tensor of order 4. It turns out that all operators of interest with short range interactions (e.g., the Heisenberg Hamiltonian) can be written in terms of $W$ tensors with small bond dimensions $m_W$. The structure of the $W$ tensors is determined by the specific model under investigation. We will provide the explicit MPO representation of various operators in what follows.

The matrix elements of MPO in such states,

$$\langle\phi|O|\psi\rangle = \mathrm{Tr}\; E^{[1]}_W(A, B) \times ... \times E^{[N]}_W(A, B), \quad (3)$$

can be expressed in terms of the (generalized) transfer matrices

$$E^{[j]}_W(A, B) = \sum_{\sigma,\sigma'} W^{[j]}_{\sigma\sigma'} \otimes (A^{[j]}_\sigma)^\star \otimes B^{[j]}_{\sigma'}. \quad (4)$$

The matrices $A$ and $B$ characterize the states $|\phi\rangle$ and $|\psi\rangle$, respectively. The Kronecker product $\otimes$ in Eq. 4 obviously produces transfer matrices of size $m^2 m_W \times m^2 m_W$. For the later use, we also define the special transfer matrix

$$E^{[j]}_1(A, B) = \sum_{\sigma,\sigma'} \delta_{\sigma\sigma'} (A^{[j]}_\sigma)^\star \otimes B^{[j]}_{\sigma'}. \quad (5)$$

One advantage of the MPO formalism used here over the formalism employed by VPC and PWE is the fact that it takes care of the structure of the effective Hamiltonian to be determined automatically (as encoded in the MPO), while the effective Hamiltonian in the VPC formulation depends structurally on the Hamiltonian of the model under consideration.

In order to find the ground state of a many-body system, one solves a standard variational problem, using the matrix elements of the MPS as variational parameters. The optimization of the variational parameters of the MPS is implemented as a local update step, which is repeated until the convergence is achieved [2]. In the MPO formalism, such a local update step amounts to the solution of a generalized eigenvalue problem

$$H^{[j]}_{\mathrm{eff}} \varphi^{[j]} = \epsilon^{[j]} N^{[j]}_{\mathrm{eff}} \varphi^{[j]} \quad (6)$$

in terms of the effective Hamiltonian $H_{\mathrm{eff}}$ and the effective normalization matrix $N_{\mathrm{eff}}$ given by

$$H^{[j]}_{\mathrm{eff}} = \sum_{kl}^{m_W} W^{[j]}_{kl} \otimes \left( \widetilde{H^{[j]}_R \cdot H^{[j]}_L} \right)_{lk}, \quad (7)$$

$$N^{[j]}_{\mathrm{eff}} = \mathbb{E} \otimes \left( \widetilde{N^{[j]}_R \cdot N^{[j]}_L} \right). \quad (8)$$

The energy of the state is obtained from $\epsilon^{[j]}$, and this value will converge to the ground-state energy eventually. In fact, we stop the iterative update procedure, if this quantity does not change any more with respect to defined convergence criteria.

The updated MPS is obtained from $\varphi^{[j]} = M_{(\sigma,l',l)}$ by a suitable partitioning of the vector into a tensor. The tilde in (7) indicates the operation $X_{(ij),(i'j')} = \tilde{X}_{(ii'),(jj')}$ for each $m^2 \times m^2$ submatrix of the bracketed quantities. As a consequence of this transposition, the effective Hamiltonian and the normalization matrix are assured to be Hermitian matrices, and the standard methods for the solution of generalized eigenvalue problems can be applied. (For open boundary conditions, the normalization matrix is unity, and only a standard eigenvalue problem needs to be solved.)

The matrices $H^{[j]}_L$, $N^{[j]}_L$ and $H^{[j]}_R$, $N^{[j]}_R$ are the products of transfer matrices from all sites to the left and to the right of the site $j$, where the MPS is updated. The $H$ matrices are obtained from generalized

transfer matrices as defined in Eq. (4), while the $N$ matrices are formed from the transfer matrices defined in Eq. (5), in both cases setting $A = B = M$ with $M$ the MPS to be determined.

In the algorithm proposed by VPC, one sweeps back and forth over the entire lattice several times updating the MPS at each site until the convergence of the energy $\epsilon^{[j]}$ is achieved. Initially, one starts from a randomly selected MPS. After each update step, the updated matrix is regauged in order to keep the algorithm stable. The standard regauging procedure, which assures the relation

$$\sum_{\sigma} B_{\sigma}^{[j]} B_{\sigma}^{[j]\dagger} = 1 \tag{9}$$

after each update step is described in more details in Refs. [3] and [4].

Similarly, excited states will be constructed iteratively by finding the lowest state in the space orthogonal to the space spanned by the states already found. We will denote the matrices of these MPS by $\Phi_{\sigma,k}^{[j]}$, where $k$ enumerates these states ($k = 0$ for the ground state, $k = 1$ for the first excited state, *etc.*). It was pointed out in Ref. [4] that this construction can also be implemented iteratively as an update step by locally projecting to the orthogonal subspace. Here, we need to determine the local projection operator $P^{[j]}$ with the property

$$P^{[j]} Y_k^{[j]} = 0 \quad \forall\ k \tag{10}$$

with

$$Y_k^{[j]} = \widetilde{O_R^{[j]} \cdot O_L^{[j]}} \Phi_k^{[j]} \ \text{ and } \ Y_k^{[j]\dagger} \cdot Y_m^{[j]} = 0 \ \text{ if } \ k \neq m. \tag{11}$$

Here, the spin and $m$ indices of the $\Phi_{\sigma,k}^{[j]}$ matrices are suitably combined to form a vector. For simplicity, we will use the same symbol $\Phi^{[j]}$ for these vectors (see the analogous definition of $\phi^{[j]}$ above).

The matrices $O_L^{[j]}$ and $O_R^{[j]}$ are products of transfer matrices as defined in Eq. (5) from all sites to the left and to the right of the site $j$, respectively, and setting $B = M$ and $A = \Phi_k$ with $M$ the (excited) MPS to be determined. The update procedure for these matrices is implemented as a generalized eigenvalue problem (see Eq. (6)) for the projected effective Hamiltonian $P^{[j]} H_{\text{eff}} P^{[j]\dagger}$ and the normalization matrices $P^{[j]} N_{\text{eff}} P^{[j]\dagger}$. The (local) projection operator $P^{[j]}$ will be constructed according to Eq. (10) by finding a set of vectors orthogonal to the calculated $Y_k^{[j]}$. A standard numerical orthogonalization routine is employed for this purpose.

## 3. Efficient Implementation

In order to implement the local update steps just described, one needs to calculate various products of transfer matrices. These are standard matrix products. However, depending on the bond dimension of the MPS and MPO, they may be numerically expensive. Naively, the multiplication of two transfer matrices (4) requires $O(m^6 m_W^3)$ operations, which may be reduced in view of the structure of the transfer matrices to $O(m^5 m_W^3)$. In analogy to the proposal by PWE, we will now describe a procedure to reduce this operational count further. This reduction occurs due to the structure of the $W$ tensors and, in particular, for products of transfer matrices with many factors, i.e., long products. Here (unlike Ref. [3]), we consider the products of transfer matrices in terms of MPSs and MPOs,

$$E_W^{[1]}(A,B) \times ... \times E_W^{[l]}(A,B) = \sum_{k=1}^{m_W m^2} \sigma_k\ u_k \otimes v_k^{\dagger}. \tag{12}$$

As was pointed out by PWE, the sum over $k$ may be cut at rather low values, which has two reasons for the generalized transfer matrices. First, the rank $m_S$ of the transfer matrices is in many practical situations lower than $m_W m^2$. This reduces the upper limit of the sum to $m_S$. For example, as will be indicated below, the rank of the transfer matrices for the Ising or Heisenberg model is $2m^2$ and not $3m^2$ or $5m^2$, respectively, as expected naively. This reduction of the summation limit is exact and does not depend on the product length.

However, for long products, the upper limit may be reduced to very low values due to the fact that only very few singular values $\sigma_k$ in expansion (12) are significantly different from 0. For the ground state calculations of chains with about 100 sites and $m = 10$, one needs to consider only about 20 singular values. This is demonstrated for the Heisenberg model in Fig. 1. This figure corresponds to Fig. 1 of Ref. [3] and shows rather similar results for $N_L$. Here, we also plot the singular values of $H_L$, and we see that only a few more singular values than those for $N_L$ are needed.

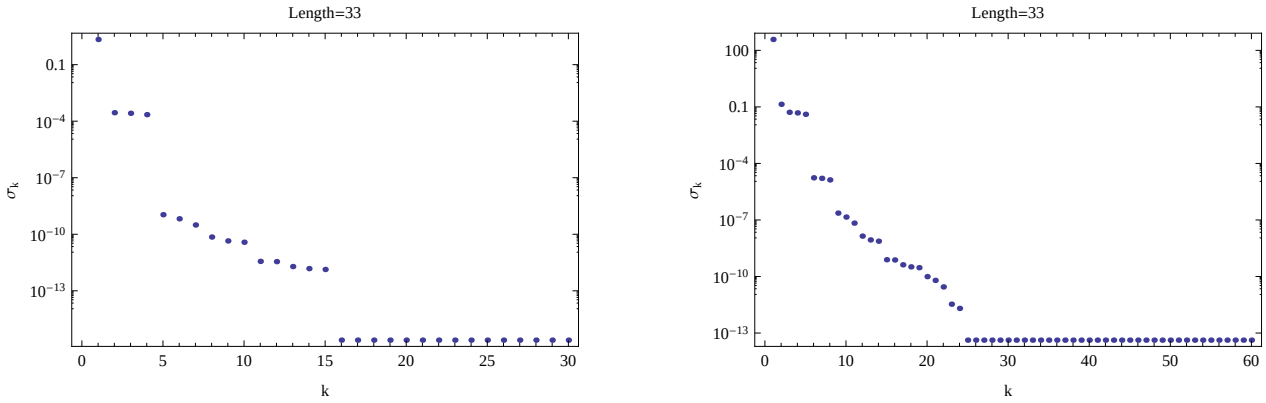


***Fig. 1.*** Distribution of the singular values of products of transfer matrices for $m$=10, $N_L$ (left) and $H_L$ (right), with 33 terms, which is the minimum number of terms in our calculation for $N = 100$ sites on a ring with homogeneous nearest-neighbor Heisenberg interactions

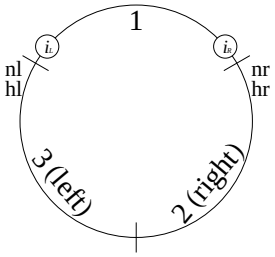


***Fig. 2.*** Circular algorithm for a ring with $N$ sites: the ring is partitioned into three sections. Updating only happens in one of them, so that we always deal with the products of transfer matrices with minimum length $N/3$. For further discussion, see the main text

(Beyond a certain limit, the singular values are set to an irrelevant small constant by our computer implementation.)

In order to utilize this feature for the local update algorithm described in the previous section, one needs to implement the algorithm in such a way that only sufficiently long products of transfer matrices occur during the update process. Therefore, one cannot use the standard sweeping procedure since the "short" products of transfer matrices occur at the turning points of the sweeps. Following PWE, we implement the algorithm as a circular update procedure. The ring of sites is separated into three sections as shown in Fig. 2, and the update process occurs always in the "active" section. The algorithm is then implemented in 3 basic steps:

1. (Initialization step) Start from some initial randomly created matrix product state $|\psi\rangle$, as defined in Eq. (1). The bond dimension of all matrices ($j = 1, ..., N$) is $m$. Partition the set of matrices into three sections, as shown in Fig. 2.

Initialize section 3 with a singular value decomposition (SVD) of the products of generalized transfer matrices defined in Eqs. (4) and (5) and store this SVD in the tensors `hl` and `nl`, respectively. Initialize section 2 with an SVD of the products of transfer matrices and store this SVD in the tensors `hr` and `nr`.

2. (Update step) Goto section 1. Initialize each site of section 1 with the appropriate product of transfer matrices moving counter-clockwise starting from the product corresponding to section 2. Then update and regauge the MPS in section 1 moving clock-wise using the previously calculated products of transfer matrices. Updating means solving the generalized eigenvalue problem described above for each site. (One immediately obtains an SVD of the products of transfer matrices *inside* the updated section by multiplication to the SVD of the previous site, i.e., one does not need to calculated an SVD at each update step. This is an important advantage of the algorithm using MPS and MPO.)

Finally, copy the tensors `nl` and `hl` on the tensors `nr` and `hr` and calculate the SVD of the product of transfer matrices of section 1 with the just updated MPS matrices and store this SVD in the tensors `nl` and `hl`.

3. Goto section 2 and do analogous calculations as described for section 1 above. Continue with further

steps moving clockwise to the neighboring section until convergence is achieved.

An important prerequisite for the implementation of the algorithm is an efficient SVD. This has been described in Ref. [3], but we have a few remarks: let $M$ be a product of transfer matrices. Then, according to the procedure outlined in Ref. [3], one has to form the products of these matrices $M$ with some matrices $x$ and $y'$ of size $p \times m^2$, e.g., $y = xM$ and $z = My'^T$. In order to do this efficiently, one *must not* calculate the matrix $M$ explicitly, but rather multiply each transfer matrix in $M$ recursively to $x$ or $y'$ starting from one or the other end of the sequence of factors in $M$. Then the multiplication of $M$ to the matrices $x$ or $y'$ can be done in $O(Npm^3)$, where $N$ is the number of transfer matrices in $M$.

Similar steps, as is outlined above for ground state calculations, are required for the determination of excited states. In other words, for each excited state, we use the same algorithm searching for the optimal MPS in the space orthogonal to the states already found. We have implemented the described algorithm within a few pages of *Mathematica* code.

## 4. Matrix Product Operators

In order to apply the algorithm developed above to specific problems, we must define the relevant degrees of freedom, the size of the local Hilbert space, and the interaction in terms of a suitable MPO. Once this MPO is defined, the implementation of the algorithm takes care of the details of the calculation.

The simplest examples to be considered are spin models, e.g. the spin-$S$ unisotropic Heisenberg Hamiltonian in an external magnetic field $B$,

$$\mathcal{H} = J \sum_{i=1}^{N} S_i^x \otimes S_{i+1}^x + S_i^y \otimes S_{i+1}^y +$$

$$+\Delta S_i^z \otimes S_{i+1}^z - B \sum_{i=1}^{N} S_i^z, \tag{13}$$

with the exchange interaction $J$, and the unisotropy $\Delta$. In what follows, we will set $J = 1$. The Hamiltonian is written in terms of the spin operators $S_i = \frac{1}{2}\sigma_i$. For spin-$\frac{1}{2}$, the $\sigma$ matrices correspond to the standard Pauli matrices. Periodic boundary conditions correspond to setting $N + 1 \mapsto 1$.

Construction of the MPO for periodic boundary conditions is not difficult,

$$W^{[1]} = \begin{pmatrix} -BS_z & S^x & S^y & S^z & e \\ 0 & 0 & 0 & 0 & S^x \\ 0 & 0 & 0 & 0 & S^y \\ 0 & 0 & 0 & 0 & \Delta S^z \\ 0 & 0 & 0 & 0 & 0 \end{pmatrix}, \tag{14}$$

$$W^{[i]} = \begin{pmatrix} e & 0 & 0 & 0 & 0 \\ S^x & 0 & 0 & 0 & 0 \\ S^y & 0 & 0 & 0 & 0 \\ S^z & 0 & 0 & 0 & 0 \\ -BS_z & S^x & S^y & \Delta S^z & e \end{pmatrix} \quad \text{for } i = 2, ..., N$$

with $e$ to be a unit matrix. The local single-body Hilbert space has dimension $2S+1$, and the bond dimension is $d_W = 5$. However, the rank of the transfer matrices, which determines the cost of the calculation, is not $5m^2$, as expected naively, but only $2m^2$. The first matrix has a different structure as compared with the other matrices in order to fulfill the required boundary conditions.

For a bilinear-biquadratic spin-$S$ ring with the Hamiltonian

$$\mathcal{H} = \sum_{i=1}^{N} a\mathbf{S}_i \otimes \mathbf{S}_{i+1} + b(\mathbf{S}_i \otimes \mathbf{S}_{i+1})^2, \tag{15}$$

one easily finds an explicit MPO representation with the bond dimension $d_W = 14$. Here, again, the rank of the transfer matrices is not $14m^2$ but only $2m^2$, which reduces the calculational cost significantly.

The calculation of matrix elements for observables (e.g., the magnetization or correlation functions) is straightforward in the MPS representation either with an MPO representation of the operators or without. For these calculations, one may take advantage of the fact that such calculations are just products of transfer matrices (see Eq. (3)) and use expansion (12) for long products. In the present paper, we will use this feature for the calculation of the variance of the Hamiltonian, as is discussed in the next section.

## 5. Applications

In order to test the implementation of the proposed algorithm, we start out with calculations of the isotropic Heisenberg model also studied in Ref. [3]. Of course, it is easy to calculate the energy spectra for small systems (10–50 sites) using our implementation, and we have calculated up to 30 excited states

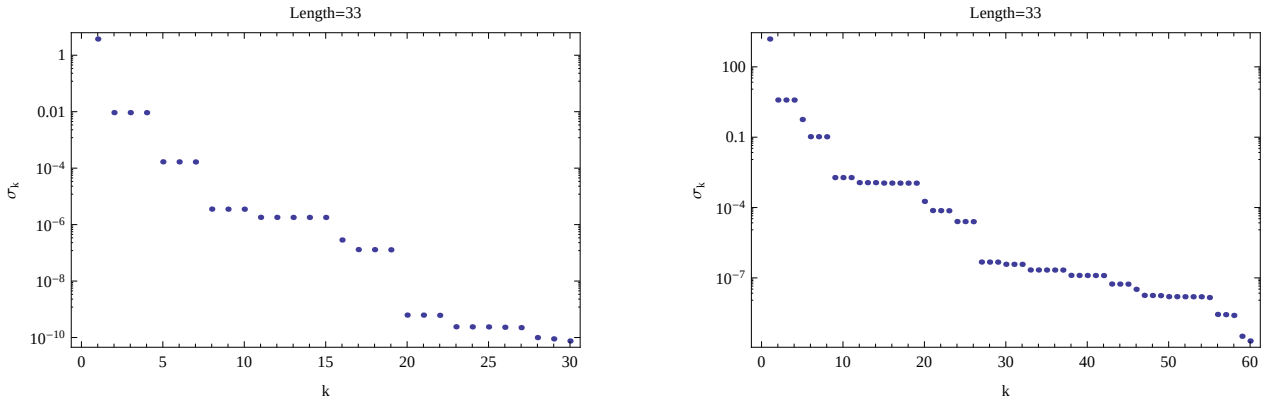


***Fig. 3.*** Distribution of the singular values of products of transfer matrices for $m = 30$, $N_L$ (left) and $H_L$ (right), with 33 terms, which is the minimum number of terms in our calculation for $N = 100$ sites on a ring with homogeneous nearest-neighbor Heisenberg interactions

for such systems. However, then one must consider most or all of the singular values in the expansion of the transfer matrices. In order to take advantage of a significant reduction of the number of singular values, the system size should be about 100 sites or more, and we present results for systems with 100 sites in this paper.

In order to run such calculations, three important parameters, which determine the precision of the results, must be set: the bond dimension $m$, the number of singular values to be included in the expansion of various transfer matrices $p$ and $p'$, and the number of update steps $N_u$, where $p$ and $p'$ are the numbers of singular values retained in the expansions of the $N_X$ matrices and the $H_X$ matrices, respectively.

Of course, a large $m$ is desirable. However, the algorithm scales at least with $p'm^3N$, so we are presently limited to about $m = 50$ in practice. We shall demonstrate below that the number of singular values to be taken into account increases with $m$, and one must be careful not to take too few terms in expansion (12). Unfortunately, the convergence of the update process is rather slow close to the minimum of the energy. Therefore, for high-precision results, we need more and more update steps. Usually, we choose their number dynamically by observing the change of the calculated energy within one sector. If this change (averaged over the whole section) is below a certain limit, we stop the update process.

One purpose of the present calculations is to gain experience in the parameter setting for $m, p, p'$, and $N_u$ in order to find, e.g., the Haldane gap in a spin-1 ring with sufficient precision. The gap is obtained from a difference of two large energies of similar values, so the two energies must be calculated with rather good precision. (Let us note parenthetically that the $m$ required in the present algorithm is significantly smaller than the corresponding quantity in standard DMRG calculations.)

In Fig. 3, we show the distribution of singular values of the transfer matrices obtained at the end of a calculation with $m = 30$ for the isotropic spin-1 Heisenberg model; i.e., the calculations shown in Fig. 1 and Fig. 3 only differ in the choice for $m$. From a comparison of these results, one concludes that if we increase $m$, we also need to increase the number of singular values to be taken into account. Our experience shows that the necessary increase is quite significant, depending on the $m$ one wants to use for a particular calculation. This fact was not mentioned in Ref. [3]. However, after this paper was nearly completed, we became aware that a similar observation was made in Ref. [5] for the standard PWE algorithm without MPO.

The MPS-MPO formalism employed here allows us to straightforwardly test how well the calculated MPS approximates an eigenstate of the Hamiltonian. To this end, we calculate the variance

$$\Delta\mathcal{H} = \langle\mathcal{H}^2\rangle - \langle\mathcal{H}\rangle^2, \tag{16}$$

which should be zero for an eigenstate. Since, from the algorithm, we obtain an explicit representation of the state, we can, at least in principle, easily evaluate this quantity, if we find a suitable MPO representa-

*Table 1.* **Ground-state energy $E_0$, first excited state energy $E_1$, and Haldane gap $E_1 - E_0$ for an isotropic spin-1 Heisenberg ring of $N = 100$ sites. $\Delta/E$ is the relative difference between our calculated result and the value calculated by DMRG given in Ref. [3]**

| $m$ | $E_0/N$ | $\Delta/E$ | $E_1/N$ (3) | $E_1 - E_0$ |
|---|---|---|---|---|
| 10 | –1.40122726344 | $1.83\ 10^{-4}$ | –1.39621210860 | 0.50153 |
| 20 | –1.40145874749 | $1.47\ 10^{-5}$ | –1.39730198769 | 0.41566 |
| 30 | –1.40148324293 | $5.83\ 10^{-7}$ | –1.39736419879 | 0.41192 |
| 40 | –1.40148390219 | $9.73\ 10^{-8}$ | –1.39737237500 | 0.41115 |
| DMRG [3] | –1.4014840386(5) | – | – | |
| DMRG (infinite) [1] | –1.40148403897 | – | –1.39737901875 | 0.41050 |

*Table 2.* **Ground-state energy $E_0$, first excited state energy $E_1$, and gap $E_1 - E_0$ for a biquadratic spin-1 Heisenberg ring of $N = 100$ sites ($a = 0$, $b = -1$ in Eq. (15)). $\Delta/E$ is the relative difference between the Bethe ansatz results and the numerical values obtained. ($p = 30$, $p' = 60$), $\Delta H$ is the variance of the Hamiltonian**

| $m$ | $E_0/N$ ( $\Delta/E$ ) | $\Delta H$ | $E_1/N$ ( $\Delta/E$ ) | $\Delta H$ | $E_1 - E_0$ |
|---|---|---|---|---|---|
| 10 | –2.794 020 092 ($1.04\ 10^{-3}$) | 1.08 | –2.793 830 121 ($1.05\ 10^{-3}$) | 1.10 | 0.018 997 |
| 20 | –2.795 792 099 ($4.07\ 10^{-4}$) | 0.44 | –2.795 632 899 ($4.12\ 10^{-4}$) | 0.44 | 0.016 077 |
| 30 | –2.796 790 186 ($5.03\ 10^{-5}$) | 0.03 | –2.796 675 842 ($3.95\ 10^{-5}$) | 0.28 | 0.011 452 |
| Bethe ansatz [7] | –2.796 930 734 | – | –2.796 786 305 | | 0.014 442 |

tion of $\mathcal{H}^2$. The bond dimension of $\mathcal{H}^2$ is $m_W^2$, but its rank is often significantly lower, which is used to significantly reduce the cost for the calculation of $\mathcal{H}^2$ using expansion (12).

The results obtained so far for the isotropic Heisenberg model are summarized in Table 1. The ground-state energy is in good agreement with that reported in Ref. [3]. In addition, we show results for the first excited state, from which we determine the Haldane gap, whose value agrees with the infinite system DMRG calculations of Ref. [1] to two significant digits. Haldane [6] conjectured on the basis of a field theoretical study that generically integer spin chains are gapped, while half-integer spin chains are gapless in the thermodynamic limit. For specific examples (spin-$\frac{1}{2}$ and spin-$\frac{3}{2}$), we can confirm this numerically with our calculations.

For the ground state, we judge the precision of the obtained results by a comparison to a high-precision result obtained within DMRG as quoted in Ref. [3] and assume that this value is numerically exact for the Heisenberg ring with 100 sites. In fact, this result is quite close to the infinite system value obtained in Ref. [1].

A second interesting test of the implementation of the proposed algorithm is the biquadratic chain, Eq. (15) (with $a = 0$ and $b = -1$), investigated by Sørensen and Young [7] in detail with the use of a mapping of the biquadratic spin-1 ring to the XXZ spin-$\frac{1}{2}$ system, which can be solved, using Bethe ansatz techniques. In Table 2, we present some preliminary results for this system, using our technique, which are compared to the high-precision Bethe ansatz results of Ref. [7]. In the thermodynamic limit, one expects a doubly degenerate ground state and a small gap to the next excited state. Of course, for finite systems, the degeneracy is lifted. This system is an interesting testing ground for our numerical techniques, as there are extremely precise results available for systems up to 1000 spins. Only for such large systems, one expects to be close to the thermodynamic limit.

The results indicate good agreement with the Bethe ansatz results. However, for a high precision, one needs large $m$ (e.g., for $m = 30$, one needs about 30-60 singular values to be taken into account). The convergence of the energies at a particular $m$, depending on the precision required, may be slow. Therefore,

*Table 3.* **Energies of the half-filled ground state $E_0$ and the next higher/lower state $E_1$ of a spinless fermion ring described by Hamiltonian (17) for $N = 128$, $m = 30$, $U = 1$, and $V = 0$**

| $\phi$ | $E_0$ | $n$ | $E_1$ | $n$ |
|---|---|---|---|---|
| 0 | –63.98647233 | 64 | –63.98581164 | 64 |
| $\pi/2$ | –64.00411240 | 64 | –64.94361781 | 63 |
| $\pi$ | –64.01004832 | 64 | –64.94770847 | 63 |

we recommend to calculate firstly with a few different $m$ in order to see the $m$ dependence before the iteration with the chosen $m$ to the high precision. How well the calculated MPS approximates an eigenstate is measured by a calculation of $\Delta H$.

As a last example, we apply the proposed algorithm to a Hubbard model of spinless fermions and, in particular, to a mesoscopic ring filled with electrons pierced by a magnetic field such that persistent currents can be observed. The Hamiltonian of this system is given by

$$\mathcal{H} = -t\sum_{\ell=1}^{N}\left(c_\ell^\dagger c_{\ell+1}e^{-i\phi/N} + \text{h.c.}\right) + \\ +U\sum_{\ell=1}^{N} n_\ell n_{\ell+1} + V\, n_1\,. \qquad (17)$$

Here, $\phi$ is the magnetic flux piercing the ring, $U$ the nearest-neighbor Coulomb interaction, and $V$ the local interaction of an impurity at site 1. Here, $c^\dagger$ and $c$ are the creation and destruction operators of fermions, and $n$ is the density operator. The hopping energy $t$ will be set to 1, and the periodicity requires to set $N + 1 \mapsto 1$.

More details about this Hamiltonian and its physics may be found in Refs. [8] and references therein. The Hamiltonian is U(1)-symmetric, and the particle number is a good quantum number to label the states. Due to the impurity, the model is not homogeneous: it is one advantage of our MPS implementation that it can handle inhomogeneous problems, since it does *not* assume the translational invariance of a system.

Since we are considering spinless fermions, the local single-body Hamiltonian describes a two-level system, which is analogous to a spin-$\frac{1}{2}$ system. The matrix representations of the single-body operators read

$$c_\ell^\dagger = \begin{pmatrix}0 & 1\\ 0 & 0\end{pmatrix},\quad c_\ell = \begin{pmatrix}0 & 0\\ 1 & 0\end{pmatrix},\quad n_\ell = c_\ell^\dagger c_\ell = \begin{pmatrix}1 & 0\\ 0 & 0\end{pmatrix}. \qquad (18)$$

Together with the $2\times 2$ unit matrix, these matrices (like the Pauli matrices) form a complete set.

One then obtains the following MPO representation for this problem,

$$W^{[1]} = \begin{pmatrix}(V-\mu)n & -c^\dagger e^{-i\varphi/N} & -ce^{i\varphi/N} & Un & e\\ 0 & 0 & 0 & 0 & c\\ 0 & 0 & 0 & 0 & c^\dagger\\ 0 & 0 & 0 & 0 & n\\ 0 & 0 & 0 & 0 & 0\end{pmatrix},$$

$$W^{[i]} = \begin{pmatrix}e & 0 & 0 & 0 & 0\\ ce^{i\varphi/N} & 0 & 0 & 0 & 0\\ c^\dagger e^{-i\varphi/N} & 0 & 0 & 0 & 0\\ n & 0 & 0 & 0 & 0\\ -\mu n & c^\dagger & c & Un & e\end{pmatrix} \quad \text{for } i = 2, ..., N$$

in terms of the matrices defined in Eq. (18); the parameters of the Hamiltonian and a chemical potential $\mu$ will be discussed below. The minus signs in the first row of $W^{[1]}$ arise due to the anti-commutativity of the creation and destruction operators on different sites.

In order to study persistent currents, one needs to calculate the ground-state energy as a function of the magnetic flux and then to find the persistent current $j$ using the Hellmann–Feynman theorem, $j = -\partial E_0(\phi)/\partial\phi$.

Since experiments are usually made for systems with fixed particle number, it would be necessary to develop the algorithm in such way that it respects the U(1) symmetry of the Hamiltonian. At this stage, our implementation does not respect this symmetry. Of course, it is always possible to shift to the ground state of the sector with the desired particle number, using an appropriate chemical potential $\mu$. However, this chemical potential is usually not known, and one would need to use an iteration process to find the chemical potential such that the resulting state contains the desired number of particles. Only for half-filled systems, it is known that the required chemical potential to find the ground state equals the interaction $U$. Therefore, we concentrate here on half-filled systems and shift the spectrum accordingly.

First results are shown in Table 3 for a ring with $N = 128$ sites. In order to be able to calculate persistent currents, using the Hellmann–Feynman theorem, one must be able to precisely distinguish the ground-state energies for different $\phi$, which requires rather high-precision calculations. The energy de-

termined for the ground state agrees with the result given in Ref. [8]. We also calculate the energy of the next higher/lower state and the number of particles $n$ it contains. Clearly, the ground state is half-filled, while the next higher/lower state contains one particle less. At $\phi = 0$, one finds a degenerate ground state in the half-filled sector. (Here, our procedure to calculate "excited" states may yield even a lower lying state, since, within the spectrum, there exist states below the ground state of the half-filled sector.) For the future calculations, an implementation respecting the U(1) symmetry is desirable.

## 6. Summary

In this paper, we suggest a new version of the efficient MPS algorithm for one-dimensional systems with periodic boundary conditions. Unlike the original proposal [3], the present version uses the MPO representation. We also extend the algorithm for the calculation of excited states. We report about the first results obtained with this algorithm and investigate the necessary parameter settings in order to obtain high precision results for systems with 100 sites. The advantage of the algorithm is that one obtains an explicit representation of the many-body quantum state, which can be used then to calculate observables such as correlation functions. We will report about such calculations in a forthcoming publication.

*We thank H.G. Evertz for a helpful correspondence. M.V. Rakov thanks Physikalisch-Technische Bundesanstalt for the financial support during three short visits to Braunschweig.*

1. S.R. White and D.A. Huse, Phys. Rev. B **48**, 3844 (1993).
2. F. Verstraete, D. Porras, and J. I. Cirac, Phys. Rev. Lett. **93**, 227205 (2004).
3. P. Pippan, S.R. White, and H.G. Evertz, Phys. Rev. B **81**, 081103R (2010).
4. D. Porras, F. Verstraete, and J.I. Cirac, Phys. Rev. B **73**, 014410 (2006).
5. D. Rossini, V. Giovanetti, and R. Fazio, J. Stat. Mech. P05021 (2011).
6. F.D.M. Haldane, Phys. Lett. **93A**, 464 (1983).
7. E.S. Sørensen and A. P. Young, Phys. Rev. B **42**, 754 (1990).
8. A. Gendiar, R. Krcmar, and M. Weyrauch, Phys. Rev. B **79**, 205118 (2009).

Received 18.04.13

*М. Вайраух, М.В. Раков*

ЕФЕКТИВНИЙ АЛГОРИТМ
ДЛЯ МАТРИЧНОДОБУТКОВИХ
СТАНІВ (МДС) ЗА ПЕРІОДИЧНИХ
КРАЙОВИХ УМОВ ТА ЙОГО ЗАСТОСУВАННЯ

Р е з ю м е

Запропоновано реалізацію ефективного алгоритму для розрахунку спектра одновимірних квантових систем з періодичними крайовими умовами. Алгоритм ґрунтується на представленні квантових станів за допомогою матричних добутків (матричнодобуткові стани (МДС)) і на аналогічному представленні гамільтоніанів та інших операторів (матричнодобуткові оператори (МДО)). Він працює набагато ефективніше для систем зі 100 і більше частинок, ніж для малих квантових систем. Формалізм застосовано для розрахунку основного стану і першого збудженого стану гайзенбергового кільця зі спіном 1 та для визначення розміру зони Холдейна. Результати зіставлено з попередніми високоточними розрахунками методом ренормгрупи матриці густини (РГМГ). Крім того, розглядаються системи зі спіном 1 і біквадратною взаємодією між найближчими сусідніми частинками. Наведено перші результати застосування алгоритму до мезоскопічного хаббардового кільця безспінових ферміонів, що переносить незагасальний струм.